

SOUTHAMPTON OCEANOGRAPHY CENTRE

INTERNAL DOCUMENT No. 70

**Airflow distortion at instrument sites
on the *R.R.S. Challenger***

D I Berry, B I Moat & M J Yelland

2001

James Rennell Division for Ocean Circulation and Climate
Southampton Oceanography Centre
University of Southampton
Waterfront Campus
European Way
Southampton
Hants SO14 3ZH
UK

Tel: +44 (0)23 8059 6406
Fax: +44 (0)23 8059 6204
Email: bim@soc.soton.ac.uk

DOCUMENT DATA SHEET

AUTHOR BERRY, D I, MOAT, B I & YELLAND, M J	PUBLICATION DATE 2001
TITLE Airflow distortion at instrument sites on the <i>R.R.S. Challenger</i> .	
REFERENCE Southampton Oceanography Centre Internal Document, No. 70, 15 pp. (Unpublished manuscript)	
ABSTRACT <p>Wind speed measurements obtained from research ships are prone to systematic errors caused by the distortion of the air flow around the ship's hull and superstructure. In this report the air flow around the <i>R.R.S. Challenger</i> is simulated for a wind speed of 15 ms⁻¹ blowing directly over the bows of the ship using a 3 dimensional Computational Fluid Dynamics (CFD) model. The airflow distortion at the sonic anemometer site has been quantified. The anemometer in this study was located at the top of the foremast and experienced a small flow distortion, with the wind speed decelerated by 0.86 % and displaced vertically by 0.83 m.</p>	
KEYWORDS AIRFLOW DISTORTION, COMPUTATIONAL FLUID DYNAMICS, CFD, CHALLENGER, WIND SPEED MEASUREMENT	
ISSUING ORGANISATION Southampton Oceanography Centre University of Southampton Waterfront Campus European Way Southampton SO14 3ZH UK	
<i>Not generally distributed - please refer to author</i>	

**AIRFLOW DISTORTION AT INSTRUMENT SITES ON
THE *R.R.S. CHALLENGER***

CONTENTS

1. Introduction.....	1
2. Description of the <i>R.R.S. Challenger</i> model	1
3. Results	2
3.a The instrument location	2
3.b The vertical displacement of the flow.....	2
3.c The free stream velocity	2
3.d The effect of the flow distortion on wind speed.....	3
4. Summary.....	3
5. References	4
6. Figures.....	5
7. Appendix.....	11

AIRFLOW DISTORTION AT INSTRUMENT SITES ON THE *R.R.S. CHALLENGER*

Berry, D. I., B. I. Moat and M. J. Yelland

June 2001

1. Introduction

This report describes an investigation of the air flow around the *R.R.S. Challenger*. The Computational Fluid Dynamics (CFD) package VECTIS was used to simulate the flow of air directly over the bow of the ship. Section 2 gives a brief description of the model. The instrument location examined in this report is that of the sonic anemometer mounted at the top of the foremast and the results are described in Section 3. Section 4 gives a summary and discussion of the results.

2. Description of the *R.R.S. Challenger* model

The modelled geometry of the *R.R.S. Challenger* is shown in Figure 1 and the location of the sonic anemometer is indicated by a cross. The geometry was enclosed in the centre of a “wind tunnel”, or computational volume, 600 m long ($-300 \text{ m} < x < 300 \text{ m}$), 300 m wide ($-150 \text{ m} < y < 150 \text{ m}$) and 150 m high ($0 \text{ m} < z < 150 \text{ m}$). The centre line of the ship was parallel to the x-axis at $z = 0 \text{ m}$. A logarithmic wind profile was specified at the inlet with a 10 m wind speed of 15 ms^{-1} .

Whilst the computational solver was running the velocity was monitored at eight locations, seven abeam of the ship in the free stream flow and one near the anemometer location. Results from these monitoring points show the model had converged after 8000 time steps with the velocities at the monitoring points constant to the third significant figure. The monitoring points are shown schematically in Figure 2 and the velocity data for the last 300 time steps are shown in Figure 3. Once the model had converged a post-processing file was written for the extraction of the data throughout the computational volume. Illustrations of the output can be found in the Appendix and a full description of the data extraction and analysis method is given by Moat *et al.*, (1996).

The flow in the tunnel was examined to ensure free stream conditions existed at the sides and ends of the tunnel, i.e. that the presence of the ship did not cause a significant blockage of the flow to these regions. Figure 4a shows the variation in velocity along the length of the tunnel, between $-250 \text{ m} < x < 250 \text{ m}$, at heights of 10 m, 20 m, 30 m and 50 m on a plane at $y = 100 \text{ m}$, i.e. towards one side of the tunnel. Equivalent data were extracted from the other side of the tunnel and identical results found. Figure 4b shows the velocity data for the central section of the tunnel, directly abeam of the ship on a plane at $y = 100 \text{ m}$ and between $-30 \text{ m} < x < 30 \text{ m}$. The change in velocities along the length of the ship on this plane at heights of 10 m and 20 m are -0.007 ms^{-1} and -0.004 ms^{-1} respectively. These results show that the blockage of the tunnel is almost zero. However, since the changes are not zero, the free stream velocity for the sonic anemometer is estimated using the vertical profile of velocity about 100 m directly abeam of the instrument site, rather than at the inlet or outlet of the tunnel.

3. Results

3.a The instrument location

The location of the sonic anemometer relative to the foremast is shown in Figure 5. In the VECTIS co-ordinates system (where the origin is at the centre of the ship at sea level), the instrument position (“P” in Table 1) is;

$$\text{Sonic} \quad x = 17.58 \text{ m, } y = 0.00 \text{ m, } z = 17.99 \text{ m}$$

3.b The vertical displacement of the flow

To calculate the vertical displacement of the flow reaching the instrument site a streamline is traced from the inlet of the tunnel to the instrument site (see Figure A4 in the Appendix). Table 1 gives the co-ordinates of; “P” the sonic anemometer site, “P_{stream}” which is the point on the streamline closest to the anemometer and “P_{origin}” the origin of the streamline. It can be seen that the streamline is displaced vertically by 0.83 m by the time it reaches the approximate position of the anemometer site. The streamline misses the anemometer site in the y direction by 0.26 m because the streamline originates far upstream of the ship where the cell size is relatively large. A vertical section (constant y) of data is viewed, and the x and z co-ordinates of the origin of the streamline are adjusted until the streamline passes through the anemometer site, but no such fine adjustment is possible in the y direction. This inaccuracy in the location of the streamlines could cause errors in the calculation of the vertical displacement of up to 0.1 m.

Location	x (m)	y (m)	z (m)
P	17.58	0.00	17.99
P _{stream}	17.58	0.26	18.02
P-P _{stream}	0.00	-0.26	-0.03
P _{origin}	184.31	0.26	17.19
P _{stream} -P _{origin}			$\Delta z = 0.83$

Table 1 The vertical displacement, Δz , of the flow to the sonic anemometer.

3.c The free stream velocity

The estimate of the vertical displacement is used to obtain the free stream velocity at the anemometer site. The air parcel reaching the anemometer will have originated at a height of $(z-\Delta z)$, where z is the anemometer height, and the free stream velocity is obtained at that height on the free stream profile. The velocity of the flow at the instrument site is then compared to the free stream velocity to give the wind speed error.

Figure 6 shows part of the free stream profile near the wind tunnel wall, directly abeam of the anemometer site at; $x = 17.58 \text{ m, } y = 100 \text{ m, } 0 \text{ m} < z < 150 \text{ m}$. This indicates a free stream velocity of 14.276 ms^{-1} at a height of 17.16 m .

3.d The effect of the flow distortion on wind speed

The free stream flow has small, predictable gradients and can be estimated accurately at any given point on the vertical profile. In contrast, the flow at an instrument site can suffer from severe flow distortion and hence large gradients in the velocity field. Additionally it is not always possible to define the mesh so that the instrument is at the exact centre of a computational cell (see Moat *et al.*, 1996). Therefore the velocity at an instrument site is estimated from lines of data extracted in all three directions. Figure 7 shows the lines of data through the sonic anemometer site and the results are summarised in Table 2. The velocity error at the instrument site (of height z) is expressed as a percentage of the free stream velocity (at height $z - \Delta z$) with a positive error indicating an acceleration of the flow.

Figure 7 is also used to estimate the gradient of the velocity of the flow in all three directions at the instrument site. These rates of change provide an indication of the accuracy of the velocity error estimate and of the severity of the local flow distortion. The rates of change, per metre and per cell, for the anemometer are given in Table 3. In general the effects of the flow distortion at the anemometer site are small with a deceleration of the flow of 0.86 % and a displacement of 0.83 m. This is confirmed by the small rates of change and by the angle of the flow to the horizontal; the wind speed components suggest an angle of flow to the horizontal of 2.67° .

Instrument site	Velocity from each direction	Average velocity (ms^{-1})	Free stream velocity (ms^{-1})	% Error
Sonic	14.150(x)	14.153	14.276	-0.86
	14.149(y)			
	14.162(z)			

Table 2. Wind speed errors at the sonic anemometer site.

Instrument site	Velocity data line	Rate of change of velocity per metre (ms^{-1}/m)	Rate of change of velocity per cell ($\text{ms}^{-1}/\text{cell}$)
HS sonic	Along (x)	0.029	0.004
	Across (y)	0.003	0.00
	Up (z)	0.137	0.031

Table 3 Rate of change of velocity close to the sonic anemometer site.

4. Summary

The distortion of the air flow at the sonic anemometer site on the *R.R.S. Challenger* has been quantified for a 10 m wind speed of 15 ms^{-1} directly over the bow of the ship. The distortion of the flow is due to the ship's hull and superstructure only, since small scale structures and very local obstructions could not be modelled.

The vertical displacement (Δz) of the flow was used to obtain an effective anemometer height ($z - \Delta z$), and the wind speed error relates the actual flow at the instrument site to the free stream

velocity at this effective height. This approach is required if the wind speed data from the anemometer are used to calculate the wind stress via the dissipation method (Yelland *et al.*, 1998). The results for the anemometer are summarised in Table 4. If the actual, rather than effective, height of the instrument is used to obtain the free stream velocity then the wind speed error will change accordingly. Table 5 shows the results if the free stream velocity is calculated in this way.

The greatest source of error in the results is likely to be in the extraction of the data. Table 3 shows that the maximum variation of the velocity from one cell to the next is 0.031 ms^{-1} . This value expressed as a percentage of the free stream velocity is shown in brackets in Table 4. Overall, the anemometer site experiences a small flow distortion, with the flow decelerated by 0.86 % and raised by 0.83 m.

Instrument	Instrument height z (m)	Velocity at instrument site (ms^{-1})	Free stream velocity (at $z - \Delta z$) (ms^{-1})	% velocity error at instrument site	Vertical displacement Δz (m)	Angle of flow to the horizontal (degrees)
Sonic	17.99	14.153	14.276	-0.86 (0.22)	0.83 ± 0.1	2.67

Table 4. Summary of the results for the sonic anemometer site on the *R.R.S. Challenger*. The figure in brackets indicates the maximum rate of change of velocity per cell (expressed as a percentage of the free stream velocity).

Instrument	Instrument height, z (m)	Velocity at instrument (ms^{-1})	Free stream velocity at height z (ms^{-1})	% velocity error at instrument site
Sonic	17.99	14.153	14.317	-1.15

Table 5. The wind speed error calculated using a free stream velocity at the actual instrument height, z .

5. References

- Moat, B. I., M. J. Yelland, and J. Hutchings, 1996: Airflow over the *R.R.S. Discovery* using the Computational Fluid Dynamics package VECTIS, Southampton Oceanography Centre, Southampton, UK, *SOC Internal Report No. 2*, 41 pp.
- Yelland, M. J., B. I. Moat, P. K. Taylor, R. W. Pascal, J. Hutchings, and V. C. Cornell, 1998: Wind stress measurements from the open ocean corrected for air-flow distortion by the ship, *Journal of Physical Oceanography* **28**, 1511 - 1526.

6. Figures

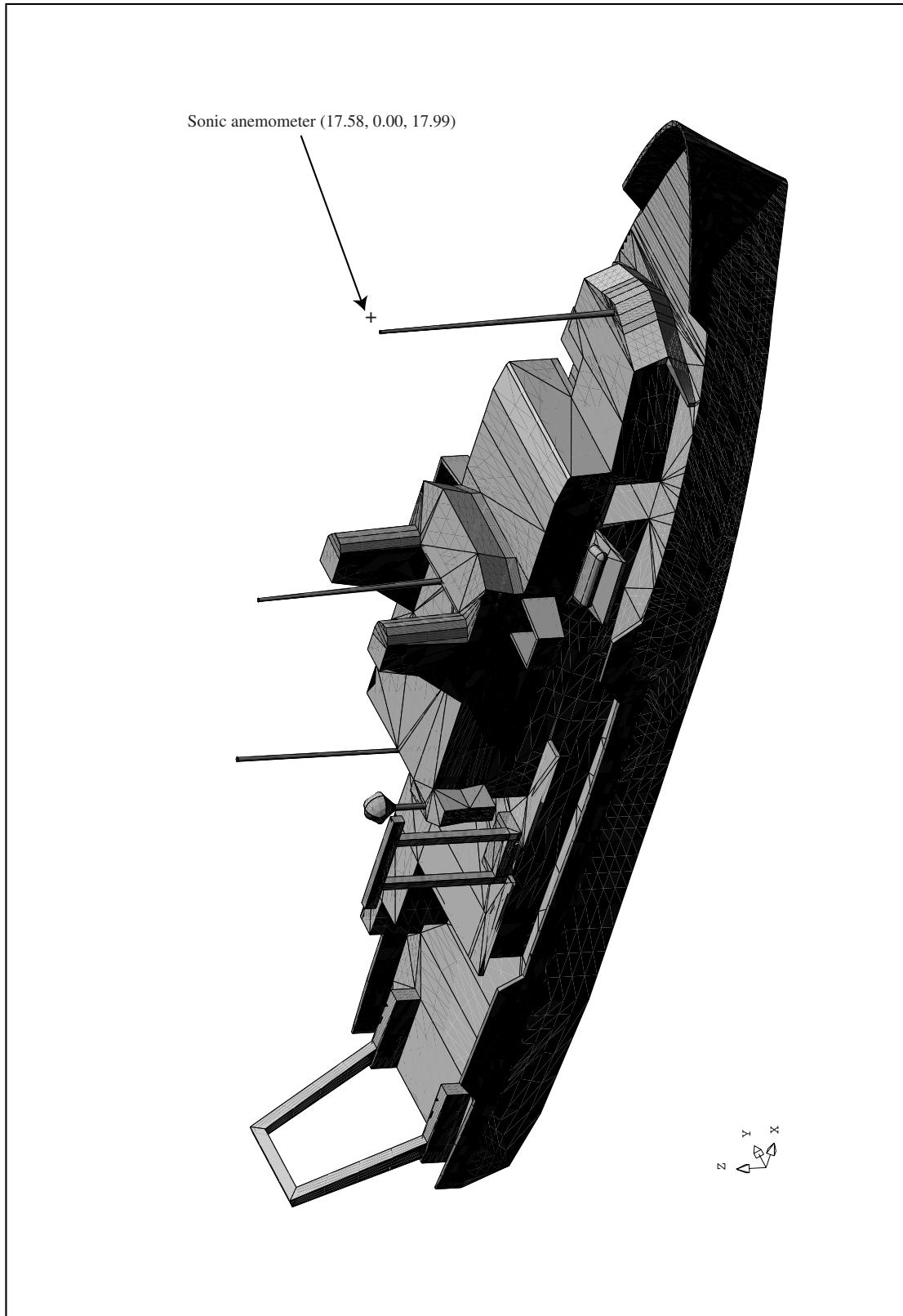


Figure 1. A three dimensional view of the model of the *R.R.S. Challenger*.

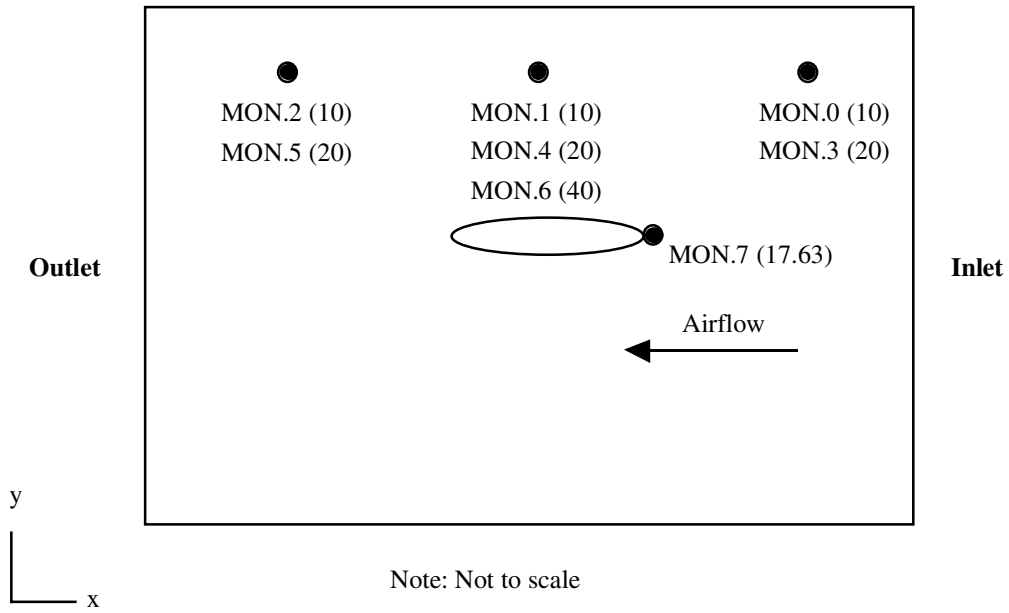


Figure 2. Schematic plan view of the wind tunnel used to simulate a flow of air over the bows of the *R.R.S. Challenger*. The monitoring points are shown by the solid circles and their heights in metres are indicated in brackets.

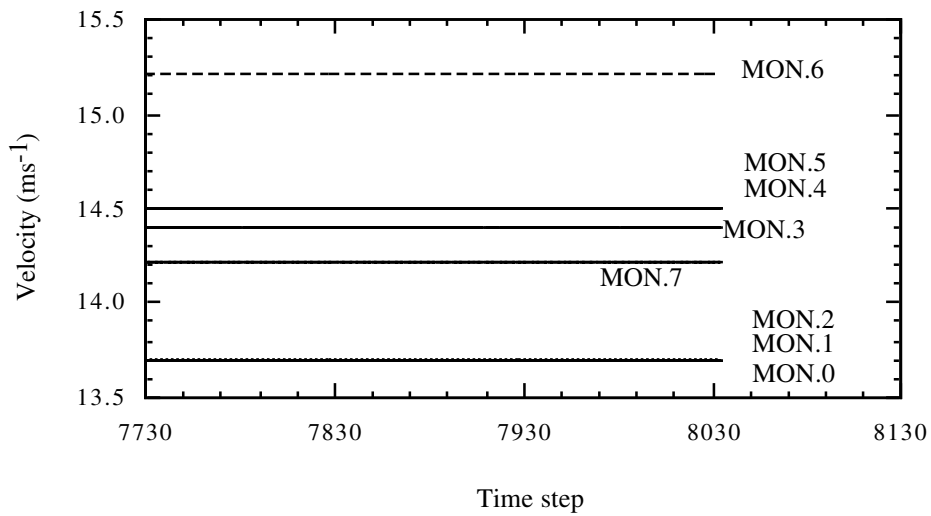


Figure 3. Velocity data for the last 300 time steps at the eight monitoring locations.

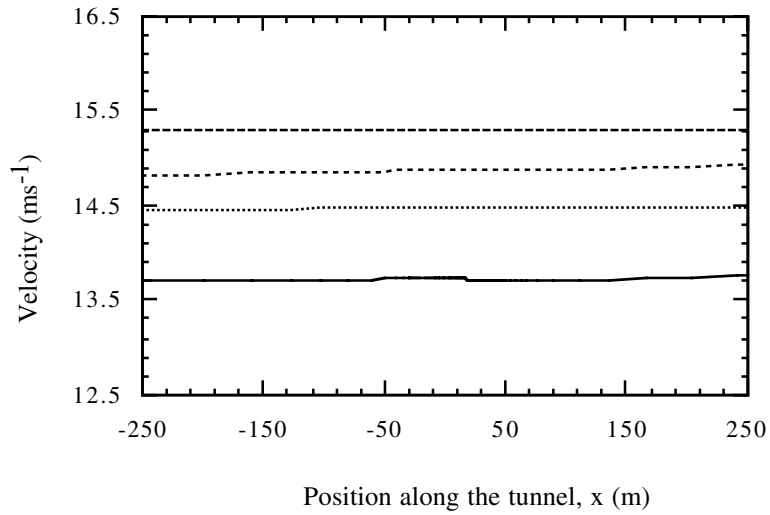


Figure 4a. Lines of velocity data along the length of the tunnel at the heights shown. The data were obtained from the free stream region on the port side of the tunnel at $y = 100$ m.

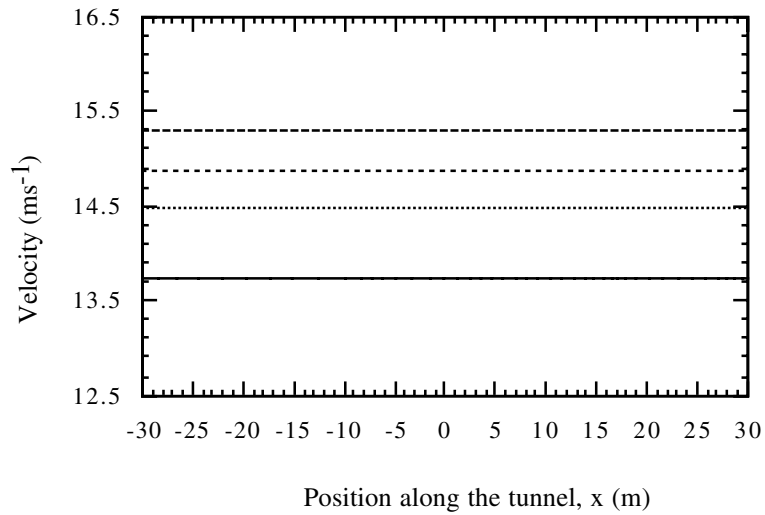


Figure 4b. As Figure 4a, showing the central portion of the tunnel only.

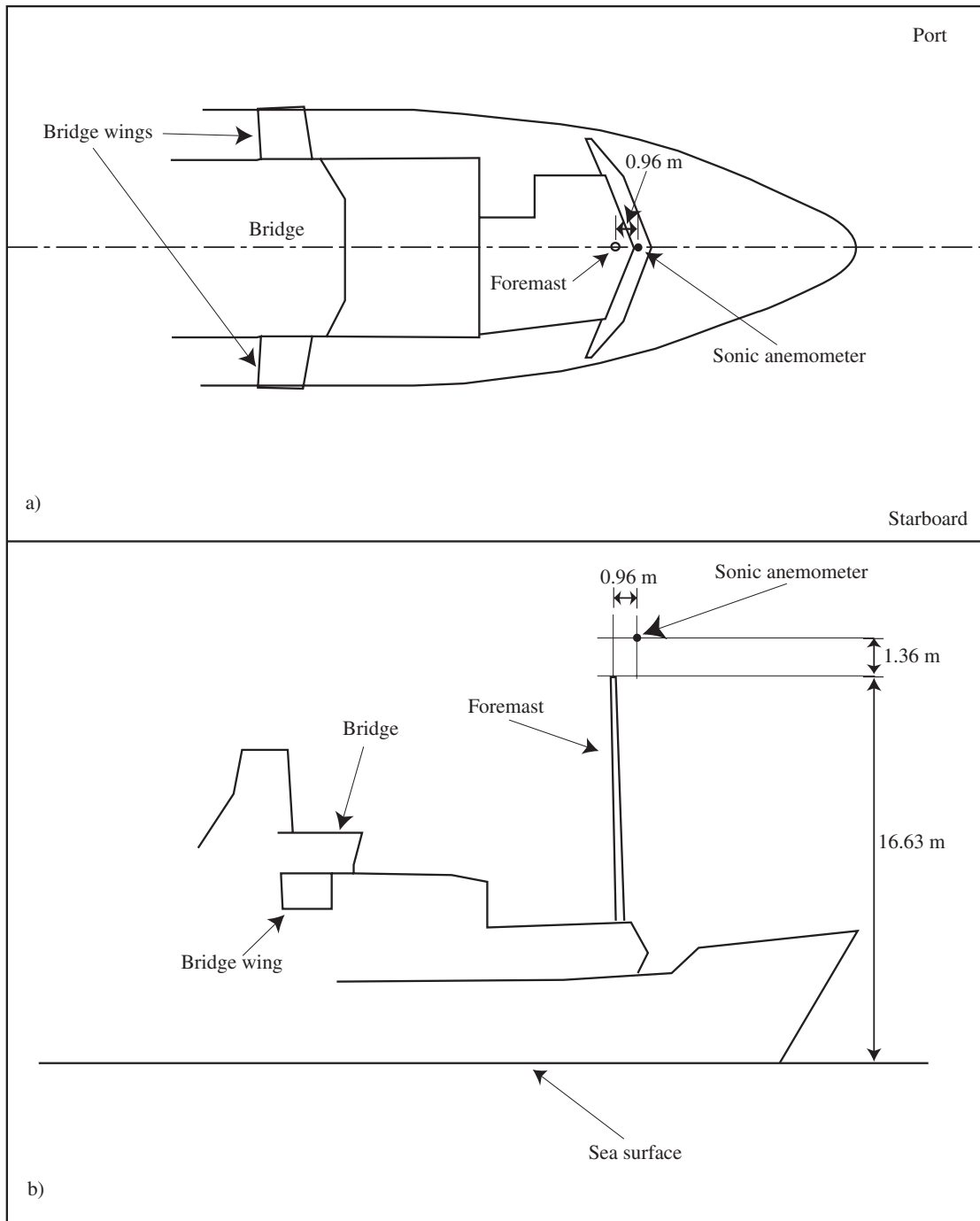


Figure 5. Schematic of the sonic anemometer position relative to the foremast; a) plan view and b) side view

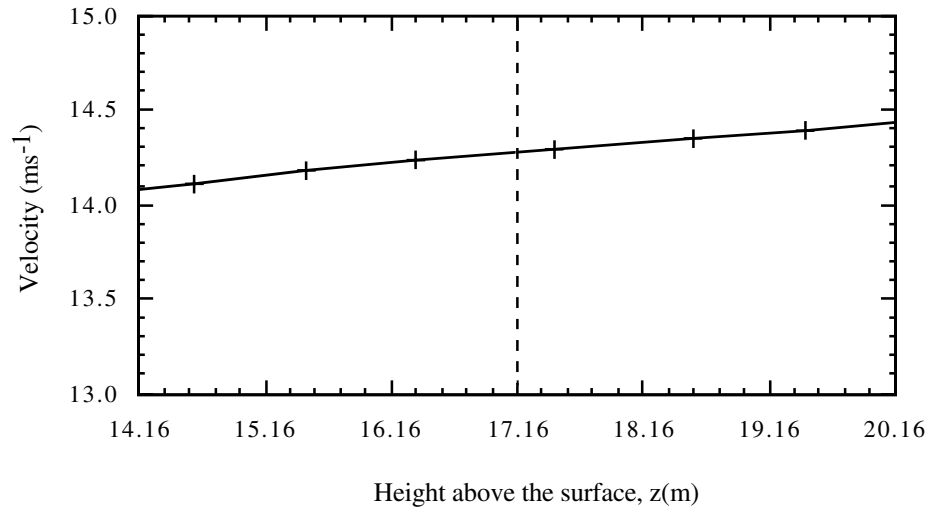


Figure 6. The vertical profile of velocity abeam of the sonic anemometer site. The dashed line indicates the height at which the air-flow originated.

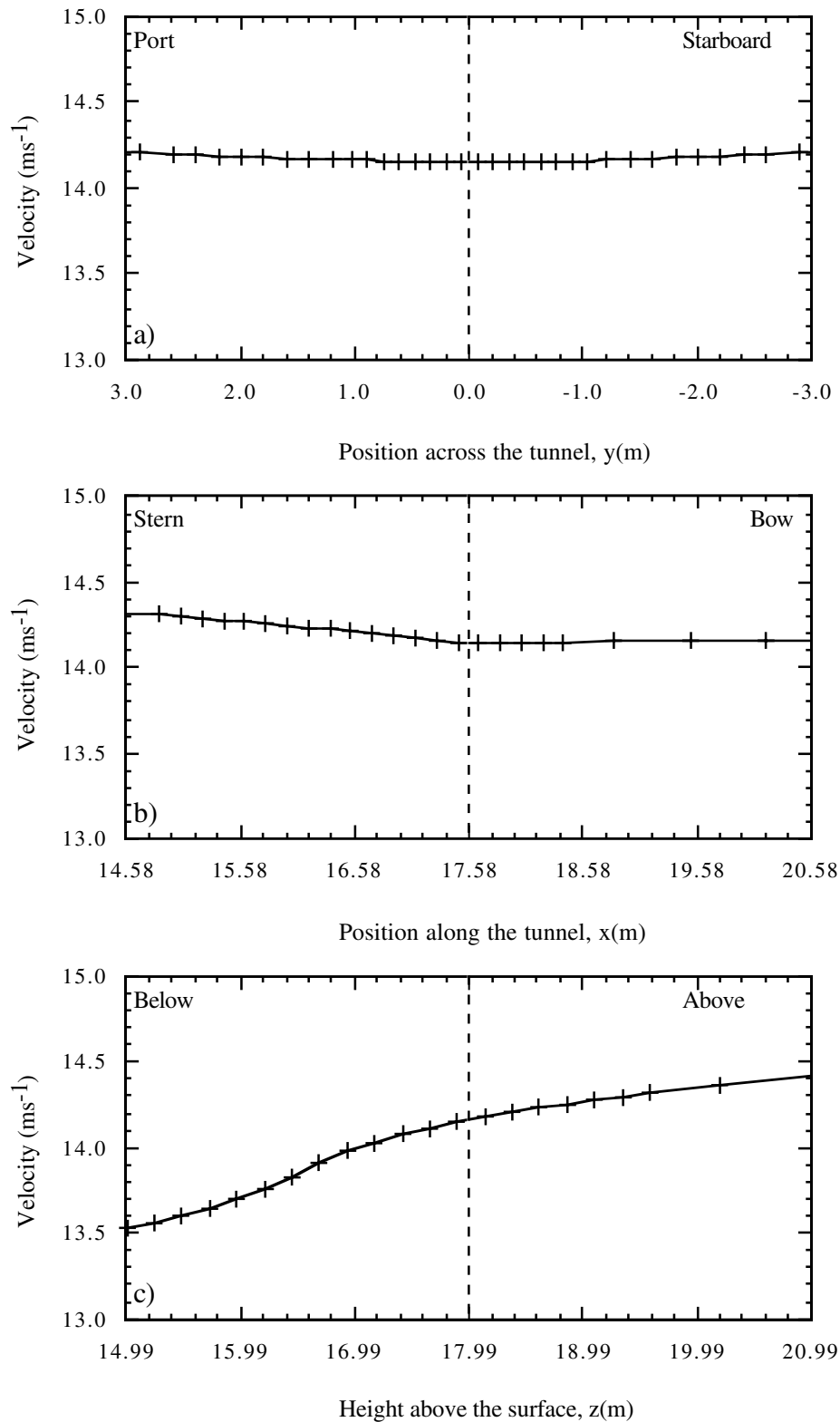


Figure 7. Lines of velocity data through the sonic anemometer position (indicated by the dashed line) in all three directions; a) across the tunnel (y); b) along the tunnel (x) and c) vertically (z).

7. Appendix

The Figures in this Appendix were generated using the VECTIS post-processing software. Each Figure shows data on a major plane, and the orientation of the plane is indicated by a red line in the small box at the top left of each Figure. The variable size of the computational cells can be seen in all the Figures.

FIGURE A1 Velocity vectors on a vertical plane through the anemometer site. The magnitude of the total velocity is indicated by the colour of the arrows. The length and direction of the arrows represent the magnitude and direction of the component of the velocity in the plane of view. Each arrow represents the result from one computational cell. The position of the anemometer is indicated by the cross and the velocity scale corresponds to 8 ms^{-1} to 16 ms^{-1} .

FIGURE A2 As Figure A1 for a vertical section across the tunnel which intersects the anemometer site (indicated by the cross).

FIGURE A3 As Figure A1 for a horizontal section through the anemometer site (indicated by the cross).

FIGURE A4 A streamline, or massless particle trace, which passes through the anemometer site (indicated by the cross).

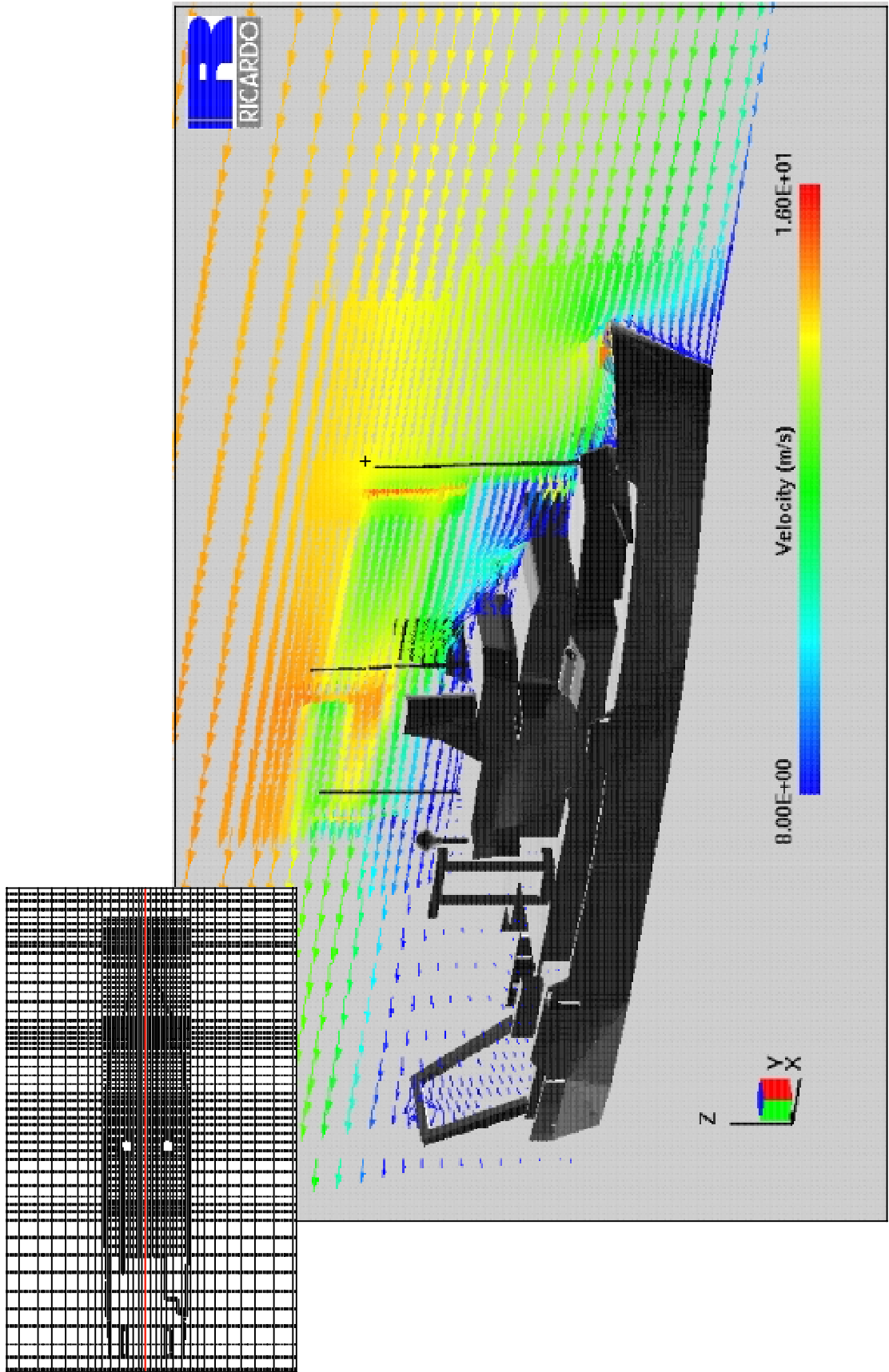


Figure A1

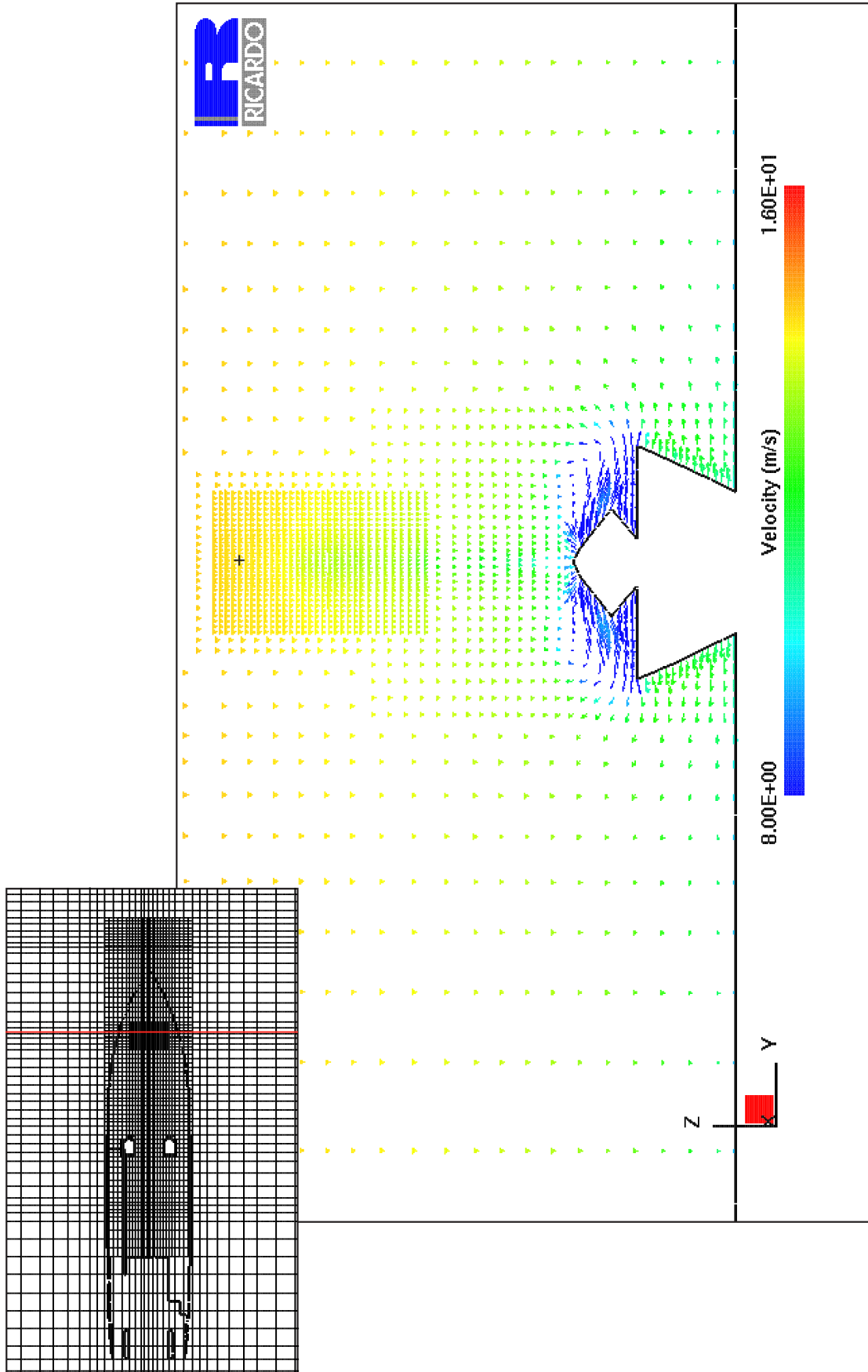


Figure A2

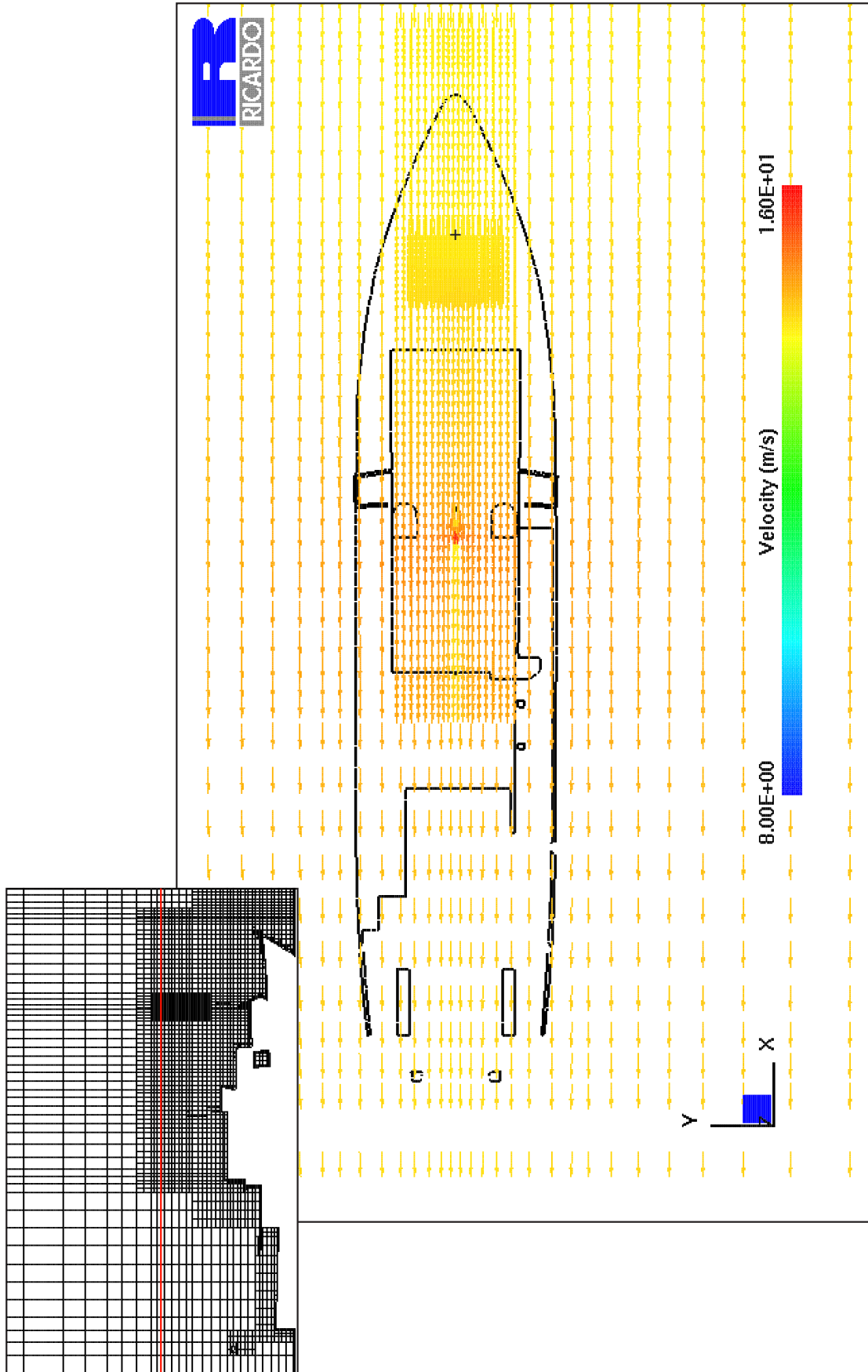


Figure A3

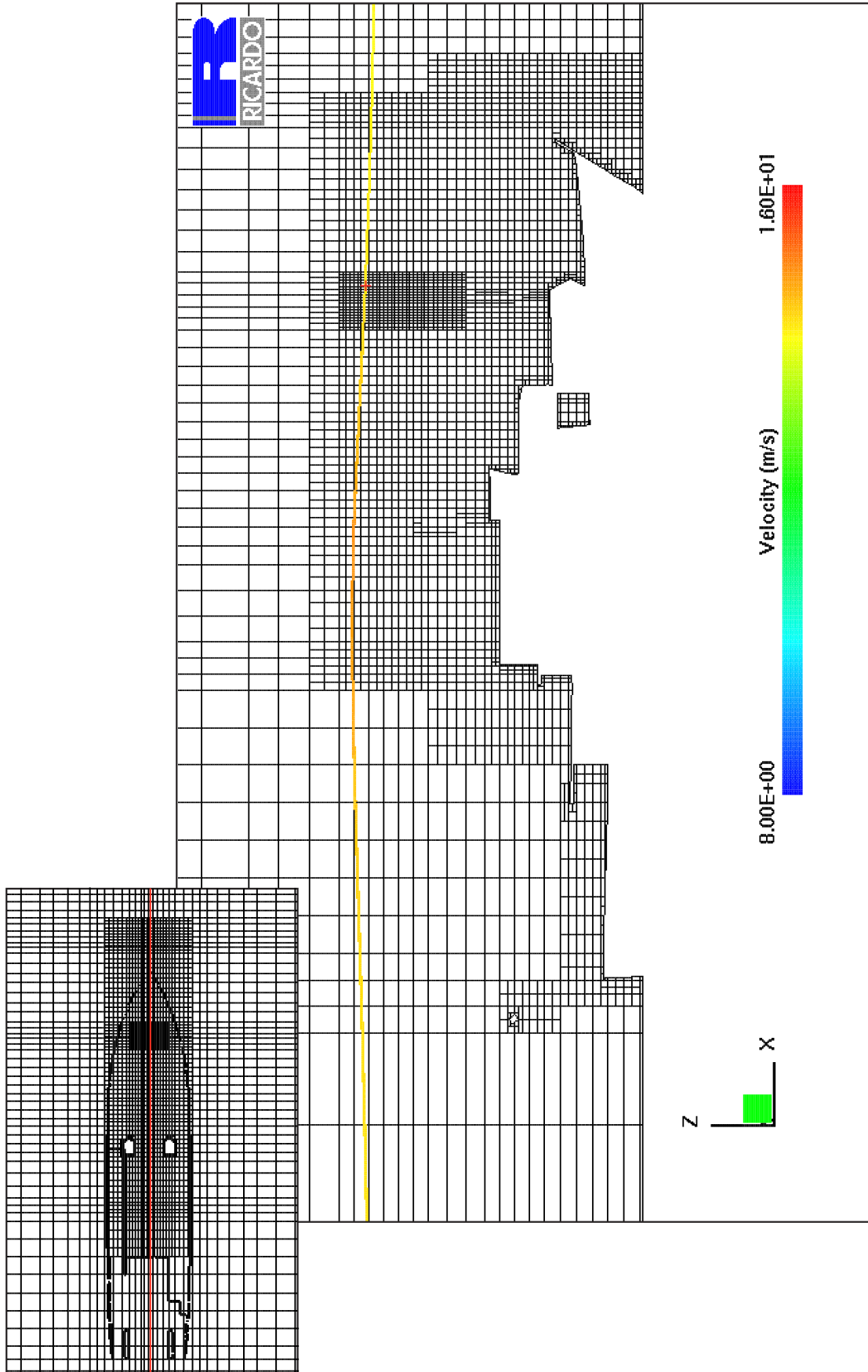


Figure A4